Journal of Chromatography A, 1371 (2014) 146–153

Contents lists available at ScienceDirect

Journal of Chromatography A

journal homepage: www.elsevier.com/locate/chroma

Ultraviolet–vis degradation of iprodione and estimation of the acute toxicity of its photodegradation products

Yannick Lassalle[a], Héla Jellouli[a], Laurie Ballerini[a], Yasmine Souissi[b], Édith Nicol[a], Sophie Bourcier[a], Stéphane Bouchonnet[a,*]

[a] Laboratoire de Chimie Moléculaire UMR-9168, École Polytechnique, 91128 Palaiseau Cedex, France
[b] Département de Génie Biologique, Université Libre de Tunis, Institut Polytechnique IP2 – 30, Av. Kheireddine Pacha, 1002 Tunis, Tunisia

ARTICLE INFO

Article history:
Received 10 July 2014
Received in revised form
14 September 2014
Accepted 17 October 2014
Available online 24 October 2014

Keywords:
Iprodione
Photolysis
Transformation products
In silico tests
In vitro tests
Vibrio fischeri

ABSTRACT

The UV–vis photodegradation of iprodione in water was investigated with a high pressure mercury lamp photoreactor. Five photoproducts of iprodione were characterized by LC–HR-MS/MS and isotopic labeling; none of them has been reported in previous studies. Three of them result from the elimination of one or two chlorine atoms followed by hydroxy or hydrogen addition while the two others are cyclic isomers of iprodione. An ICR mass spectrometer was used for by-products identification; concentrations of photoproducts were estimated with a triple quadrupole instrument, using iprodione-D_5 as an internal standard. Phototransformation mechanisms were postulated to rationalize photoproducts formation. *In silico* QSAR toxicity predictions were conducted with the Toxicity Estimation Software Tool (T.E.S.T.) considering oral rat LD50, mutagenicity and developmental toxicity. Low oral rat LD50 values of 350 mg/kg and 759 mg/kg were predicted for cyclic isomers of iprodione, compared to that of the parent molecule (2776 mg/kg). Toxicity estimations exhibited that all the iprodione photoproducts could be mutagenic while the parent compound is not. *In vitro* assays on *Vibrio fischeri* were achieved on both irradiated and non-irradiated aqueous solutions of iprodione and on HPLC fractions containing isolated photoproducts. Phenolic photoproducts were shown to be mainly responsible for toxicity enhancement with EC50 values of 0.3 and 0.5 ppm, for the bi- and mono-phenolic compounds issued from chlorine elimination.

1. Introduction

Pesticide usage is steadily increasing every year throughout the world. The Environmental Protection Agency estimates indicate a growth of 25% for the fungicides market size between 1998 and 2007 and the involved amounts raised the scientific community awareness on these molecules toxicity and stability [1]. Among these, iprodione (3-(3,5-dichlorophenyl)-*N*-isopropyl-2,4-dioxoimidazolidine-1-carboxamide) is a dicarboximide fungicide. Known as "Rovral", it was first introduced to the market in 1974 by Rhône-Poulenc [2]. It is mainly applied to prevent gray mold for ornamental cultivations [3] but also on crops, such as vineyards [4–6], apple trees [7] and tomato plants [8,9]. Its wide range of applications also includes golf greens protection [10]. It is used to protect crops from a wide range of pathogenic fungi such as *Fusarium*, *Botrytis* or *Phytophtora* [11]. Unlike most of the fungicides of this family, iprodione does not appear as an AR (Androgen Receptor) antagonist but rather as an inhibitor of steroidogenesis [12]. It alters adrenal gland function and induces interstitial cell tumors in the rat testis [13]. More recent studies have shown that iprodione could delay pubertal development in male rats [12]. According to a review of the European Commission of 2002, iprodione could be responsible for short term and long term effects such as atrophy, hyperplasia and weight change on the liver, ovary, kidney, seminal vesicles [14]. There are few data available about ecotoxicological effects of iprodione on marine organisms; they describe the effect of fungicides on aquatic fungi and microorganisms constituting interesting biomarkers [15,16]. In addition, iprodione has the capacity to diffuse in water and then is likely to cause damage on these organisms. Furthermore, Radice et al. reported that iprodione was able to produce oxidative damage in primary cultured fish hepatocytes at the concentrations of 0.3 and 0.4 mM [15]. In the agricultural field, the elimination of pesticides results from biological, chemical and/or photochemical degradation. The study of the photochemical behavior of these pollutants is thus a key element for the understanding of toxics formation [17,18]. Iprodione acts as a contact fungicide and only a fraction of the applied product penetrates the plant cuticle, thus making it very

* Corresponding author. Tel.: +33 1 69 33 48 05; fax: +33 1 69 33 48 03.
E-mail address: stephane.bouchonnet@polytechnique.edu (S. Bouchonnet).

http://dx.doi.org/10.1016/j.chroma.2014.10.051
0021-9673/

prone to receive long-term sunlight irradiation [19,20]. The curative or preventive effects of fungicides are not only based on their mechanism of action but also on their chemical properties such as solubility in water or log K_{ow}, which will define which part of the plant they will target [21,22]. Photolysis can occur directly on the plant but also on the soil, and the media will greatly impact chemical processes [17]. The dicarboximide family has been previously known to be susceptible to photocatalytic and photolytic degradation. Hustert et al. described the photodegradation of vinclozolin and procymidone catalyzed by semiconductors such as iron oxide and titanium dioxide [23]. Schick et al. proposed photodegradation pathways for vinclozonin in water and methanol–water solutions [24]. More recently, the photodegradation of procymidone was examined by Rifai et al. along with the potential toxicities of formed products using *in silico* tests [25]. Iprodione has been detected after application on crops in several studies [5,26]. No study so far has reported the quantitation of photoproducts after the application of iprodione on crops. The main objective of this work was the identification of the transformation products issued from direct photolysis of iprodione in water, in order to simulate photolysis conditions on fruits or leaves after application. It is now established that liquid chromatography coupled with high resolution mass spectrometry is a method of choice for the identification of unknown contaminants in water or food [27–29]. The analytical method preferred in this work was the combination of liquid chromatography with tandem mass spectrometry (LC–MS/MS) using a high resolution FT-ICR to detect and help identifying former photoproducts. The second goal was the evaluation of the potential toxicities of these photoproducts using *in silico* QSAR (Quantitative Structure–Activity Relationship) calculations. Finally fraction separation was achieved for each photoproduct in order to assess *in vitro* toxicities on *Vibrio fischeri* with photoluminescence comparisons.

2. Experimental

2.1. Chemicals and reagents

Iprodione (99% purity) and iprodione-D_5 were purchased from Sigma Aldrich (St Quentin Fallavier, France) and Cluzeau Info Lab (Sainte Foy La Grande, France, respectively). Their chemical structures are displayed in Fig. 1. Chromatographic grade solvents (99.99% purity), acetonitrile (ACN) and formic acid (FA), were also purchased from Sigma Aldrich. Considering the poor solubility of iprodione in water (13.9 mg/L at 25 °C) [30], solutions of iprodione and iprodione-D_5 at 100 mg/L was prepared in an ACN/water 30:70 mixture. ACN does not absorb light in the UV range (0% at 200 nm) [31]. All solutions were degased using nitrogen bubbling for 15 min and sonication for 10 min. A constant pH value of 5.5 was measured at 0, 90 and 180 min.

2.2. Photolysis experiments

Photolysis experiments were carried out using a self-made reactor equipped with a high-pressure mercury lamp (HPL-N 125W/542 E27 SC; Phillips, Ivry-sur-Seine, France) delivering radiation at wavelengths ranging from 200 nm to 650 nm. According to manufacturer data, the incident radiation flux was 6200 lm. The reactor consists in six quartz tubes of 120 mL disposed in a circle around the lamp and immerged into a sonicator (AL04-12, Advantage-Lab, Switzerland) filled with deionized water. During experiments, the reactor was regularly cooled by water circulation to avoid uncontrolled heating of the irradiated solutions and to maintain a constant temperature of 25 ± 3 °C. For each experiment, 60 mL of a solution of iprodione (see above) were used. To follow the kinetic evolution of photoproducts, a series of experiments was carried out with 25 irradiation times ranging from 0 to 180 min: 0, 2, 4, 6, 8, 10, 12, 15, 18, 22, 26, 30, 40, 50, 55, 60, 70, 80, 90, 100, 110, 120, 140, 160 and 180 min. All the irradiated solutions were analyzed by LC–MS. A reference solution of iprodione was degased, sonicated and kept 180 min at 25 °C without being submitted to irradiation. Analyses showed that iprodione did not undergo any degradation under these conditions.

2.3. LC–MS operating conditions

All the chromatographic separations were carried out on a liquid chromatography Acquity HPLC system (Waters Technologies, Saint Quentin en Yvelines, France). 10 μL of the sample were injected and separated on a C_{18} Poursuit XRs^{Ultra} 2.8 μm 100 mm × 2.0 mm column (Agilent Technologies, Les Ulis, France). Elution was performed using a 0.2 mL/min solvent flow with a gradient increasing from 40% of B solvent to 95% of B solvent in 25 min (A: water + 0.1% formic acid; B: acetonitrile + 0.1% formic acid). The gradient was then set at 40% of B solvent for the last 10 min. For structural elucidation experiments, the HPLC system was coupled with a high resolution Solarix FT-ICR 7T mass spectrometer (Bruker Daltonics, Bremen, Germany). A 1:60 split was set between the column and the ESI nebulizer in order to get a flow of 200 μl/h in the FT-ICR source. An electrospray ion source was used in the positive mode. Ions were accumulated 0.01 s in the source hexapole and 0.2 s in the collision cell with a cooling time of 0.01 s. Time of flight in the optic transfer was set at 0.5 ms with a 0.1 s dwell time. The detection parameters were set using a resolution of 512,000 pts to record ions on the m/z 100 to m/z 500 mass range, with a 0.1835 ms transient duration in the broadband mode. Four acquired scans were averaged for each spectrum, corresponding to MS or MS/MS duty cycles of approximately 1.6 s. In MS/MS experiments, the precursor ion was selected in the quadrupole with an isolation window of 4 Da and submitted to collision induced dissociation with a collision energy of 8 V. For quantitation experiments, the same HPLC system was coupled with a MS-6410 triple quadrupole (TQ) mass spectrometer (Agilent Technologies, Les Ulis, France). Chromatographic conditions were the same as those described above. The capillary, ESI cone and ion guide voltages were set at 5 kV, 600 V and 20 V, respectively. Source and desolvation temperatures were respectively fixed at 50 °C and 300 °C. Nitrogen was used for nebulization and desolvation at pressures of 16 psi and 57 psi, respectively. Given that experiments were performed in pure water and that neither

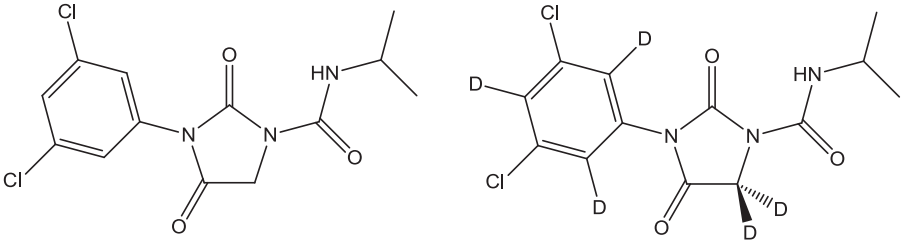

Fig. 1. Chemical structures of iprodione and iprodione-D_5.

interferent nor fragment ion was observed in the fullscan mode, experiments dedicated to fractionation control and quantitation were carried out in the selected ion monitoring (SIM) mode for a maximum sensitivity. Molecular protonated ions MH^+ were logically retained for the detection of iprodione and its photoproducts.

2.4. Grape samples analysis

Grape samples were used as test fruits for iprodione detection in a complex matrix before and after photolysis. Grape berries were evenly sprayed with a 10 ppm iprodione solution and exposed to UV–vis radiation for 1 h. The berries were then rinsed with ultrapure water, peeled and the skin and flesh were separately grinded with a manual mortal grinder. The resulting products were centrifuged at a speed of 1500 rpm for 5 min. The supernatant liquid was collected and filtrated using a 0.45 μm Gelman PTFE filter from Pall Corporation (New York, USA). The resulting solutions were directly injected in LC-ICRMS.

2.5. Sample fractionation and quantitation

Sample fractionation was necessary in order to assess the individual toxicity of each photoproduct with *in vitro* bioassay. For this purpose, the HPLC device described above was coupled with a "*Fraction collector III*" fraction collector (Waters technologies, Saint Quentin en Yvelines, France). The chromatographic column and separating conditions were the same as those used for photoproduct identification (see Section 2.3). Given the low amounts of photoproducts and the limited injection volume (10 μL), 100 runs were carried out. For each collected fraction, the solvent was removed in a XcelVap automated evaporation device (Horizon Technology, Salem, USA), 5.5 mL of water were added and the aqueous solution was homogenized before being divided into two equal parts. The first part was devoted to *in vitro* assay, the second one was used to check the purity of the photoproduct and to evaluate its concentration in the solution submitted to toxicity testing. Given that no standard of photoproduct was available, quantitation was performed using iprodione-D_5 as internal standard. It has been assumed that the main protonation sites of photoproducts being the same than those of iprodione-D_5, close response factors could be expected. Iprodione-D_5 was first added at 10 ppm in the solution to be dosed. After a first estimation based on the comparison between chromatographic peak areas of the photoproduct considered and iprodione-D_5, a second measurement was done in which iprodione-D_5 has been added at the concentration first estimated for the photoproduct. The aim of this second experiment was to reduce uncertainties by comparing chromatographic peak areas of almost the same size, assuming the LC–MS response to be linear on a short dynamic range.

2.6. In silico toxicity prediction

The Toxicity Estimation Software Tool (T.E.S.T.) is an Environmental Protection Agency online available computerized predictive system with Quantitative Structure Activity Relationships (QSAR) mathematical models [32]. T.E.S.T. has a variety of toxicity endpoints used to predict acute toxicity values from the physical properties of the molecular structure. It uses a simple linear function of molecular descriptors such as the octanol–water partition coefficient, steric and/or electronic parameters and also parameters related to the presence/absence of a given chemical group (see Eq. (1)).

$$\text{Toxicity} = ax_1 + bx_2 + c \quad (1)$$

x_1 and x_2 are independent descriptor variables and a, b and c are fitted parameters. Models for assessing toxicity solely from molecular structure are based on information-rich structural descriptors that quantify transport, bulk, and electronic attributes of a chemical structure. Besides molecular weight, the QSAR model employs size-corrected *E*-values for quantification of molecular bulk. The size-corrected *E*-values are computed from a rescaled count of valence electrons. Electrotopological state values (*E*-values) as numerical quantifiers of molecular structure encode information about the electron content (valence, sigma, pi and lone-pair), topology and environment of an atom or a group of atoms in a molecule [33]. The predicted toxicity is estimated by taking an average of the predicted toxicities from the above QSAR methods, provided the predictions are within the respective applicability domains.

2.7. Bioluminescence inhibition test of V. fischeri

In vitro tests were carried out using *V. fischeri* commercial test kits. The freeze-dried luminescent bacteria and the luminometer were purchased from Hach Lange (Hach Lange GmbH, Düsseldorf, Germany). The experimental procedure for conducting the bacterial bioluminescence assay is based on the ISO11348-3 protocol (1998). The analysis was carried out with all dilution and reagents maintained at 15 °C. A working solution of luminescent bacteria was prepared by reconstituting a vial of frozen lyophilized *V. fischeri* cells using 12.5 mL of the reagent diluent provided by the manufacturer. The reconstituted solution was equilibrated for a minimum of 15 min at 4 °C. The hydrated cell suspension is usable for several hours when kept chilled. The osmolality is adjusted in order to obtain 2 w/v% NaCl in each solution or sample. Bacterial reagents are reconstituted just prior analysis and the pre-incubation times follow standard protocols. In all measures, the percent of inhibition (*I*%) was determined by comparing the relative responses of the control and the diluted sample. Each dilution was tested in duplicate and performed at 15 °C. Dilution series of the samples to be analyzed were prepared in sodium chloride solution (2% NaCl). Different concentration intervals were used for the tested chemicals, depending on the expected EC50. For the photolyzed solutions, a larger concentration range was adopted as the EC50 values were unknown. The sample pH values were approximately 7. A fixed amount of bacteria (100 μl of the reconstituted cell suspension) was added to the dilution vials. Luminescence was measured at time zero (before addition of test solution) and then after 5, 15 and 30 min and compared to the measured value of a bacterial control. The concentration of toxicants in the test which causes a 50% inhibition of bioluminescence after exposure for 5, 15 or 30 min was designated as the EC50 value.

3. Results and discussion

3.1. Characterization of the photoproducts of iprodione

Fig. 2 displays the chromatogram (recorded in the fullscan mode) of the aqueous solution of iprodione irradiated for 60 min. Five photoproducts (PP) are detected, referred as PP1 to PP5; their retention times and mass spectra are given in Table 1. The main dissociation pathways of protonated iprodione consist in propene and isopropyl isocyanate eliminations to provide m/z 287.9931, and m/z 244.9873 ions, respectively (see supplementary material 1). Photoproduct PP1 is eluted at 11.2 min. In comparison with that of iprodione, the raw formula of PP1, determined by HR-MS measurements, shows that the two chlorine atoms have been replaced by hydroxy groups according to the mechanism suggested in Fig. 3. PP2, eluted at 19.0 min, has a molecular weight of 311 amu. The isotopic distribution and the exact mass of MH^+ ions show that a chlorine atom has been replaced by a hydroxy group. Eluted at

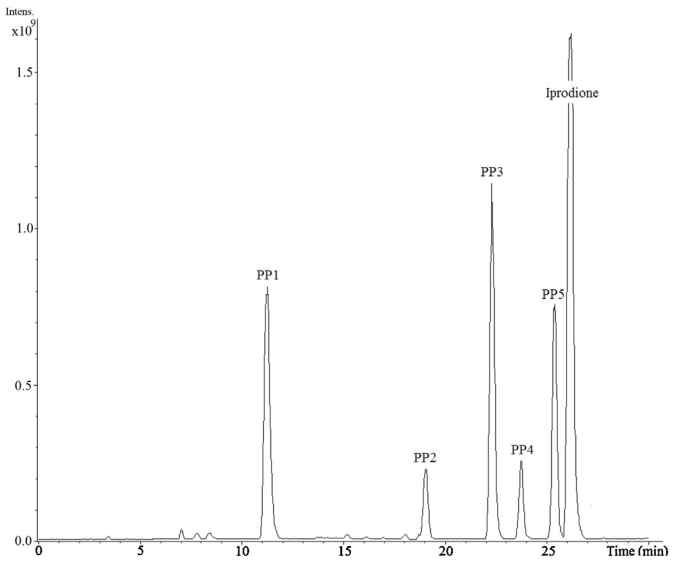

Fig. 2. LC–MS chromatogram of the aqueous solution of iprodione irradiated for 60 min (ESI in the positive mode, fullscan detection).

22.3 min, PP3 results from elimination of a chlorine atom from iprodione followed by hydrogen addition, by a mechanism analogous to those proposed for the formation of PP1 and PP2 (see Fig. 3). Photoproducts PP4 and PP5, eluted at 23.8 and 25.4 min, respectively, have the same molecular weight of iprodione. In mass spectrometry, the protonated molecular ions of PP4 and PP5 both dissociate to provide ions at *m*/*z* 244.9873 and *m*/*z* 287.9931 with raw formula analogous to those of fragment ions from protonated iprodione (Table 1). The presence of both ions indicates that the non-cyclic part of the molecule was not affected in the formation of PP4 and PP5 (supplementary material 1). Consequently, we suggested that PP4 and PP5 correspond to cyclic isomers of iprodione, resulting from the formation of a C—O bond between a carbon atom of the aromatic ring and one of the oxygen atoms of the adjacent carbonyl functions (see Fig. 3). We attribute the structure PP5 to the last eluted cyclic isomer because it appears to be the less hydrophilic one. Furthermore, compared to iprodione which elutes with a very close retention time, this structure kept the capability for a hydrogen bond between the NH function and a carbonyl group. Both reaction pathways suggested in Fig. 3 for the formation of PP4 and PP5 involve close transition states and thus similar activation energies but a hydrogen bond between a secondary amine and the oxygen atom of a carbonyl group is expected to be significantly stronger than a hydrogen bond between a secondary amine and the oxygen atom of an ester function. Consequently, the structure postulated for PP5 was assumed to more stable than that of PP4. This is in agreement with the higher relative abundance of PP5 (four times that of PP4 after 180 min of irradiation) in the irradiated solution (see Fig. 4). All the suggested structures are in agreement with the shifts observed for the *m*/*z* ratios of protonated photoproducts of iprodione-D_5: 5 amu for PP1 to PP3, 4 and 5 amu for PP4 and PP5.

Supplementary material related to this article can be found, in the online version, at http://dx.doi.org/10.1016/j.chroma.2014.10.051.

3.1.1. Kinetics data and persistency

After irradiation, 20 μL of an aqueous solution of iprodione-D_5 at 50 mg/L were added to each sample as an internal standard to evaluate the relative amounts of iprodione and photoproducts using LC–MS. The relative amount of iprodione in the irradiated solution is plotted as a function of the irradiation time in supplementary material 2, which shows that about 50% of the initial amount of iprodione was still detected after 180 min of irradiation. The relative amounts of photoproducts are plotted as a function of the irradiated time in Fig. 4. In a general manner, the formation of all photoproducts begins as soon as the solution is irradiated. The relative amounts of PP2 and PP3 rapidly increase in the same way during the first 25 min. The concentration of PP2 reaches a maximum at 25 min before decreasing. This decrease probably corresponds to the phototransformation of PP2 into PP1, as suggested in Fig. 3. The steady decrease in PP1 after 60 min was assumed to result from phototransformation of PP1 into compounds at concentrations too low to be detected in LC–MS. Phenolic compounds are known to be sensitive to oxidation in the presence of oxygen and light. The relative amounts of isomers PP4 and PP5 logically increase in the same way all along the experiment. PP3 and PP5 remain the most abundant compounds at the end of irradiation; they do not seem to degrade and are likely the ones to be mainly present in environmental samples. Unfortunately, no real samples of fruits treated with iprodione were available for the present study. Grape samples treated with a commercial preparation containing iprodione were irradiated under laboratory conditions and analyzed as described in Section 2.4. Iprodione was detected in skin and flesh of non-irradiated grapes and all the photoproducts were detected in skin and flesh of irradiated berries. Nevertheless, they were not real environmental samples submitted to solar irradiation and this result does not provide evidence that these photoproducts would be formed under field conditions.

Supplementary material related to this article can be found, in the online version, at http://dx.doi.org/10.1016/j.chroma.2014.10.051.

3.2. In silico toxicity prediction

To our best knowledge, no data on the toxicity of iprodione degradation products has been reported to date. *In silico* tests were performed using the toxicity simulation program described in Section 2.6. Results for iprodione and its photoproducts are presented in supplementary information file SI 3. Oral rat LD50 endpoint indicates the amount of chemical in mg/kg body weight that would cause 50% of a test population of rats to die after oral ingestion. The oral rat LD50 estimated for iprodione (2776 mg/kg) is coherent with literature data reporting values in the range 2000–2500 mg/kg [34,35]. This value corresponds to a slight toxicity according to Hodge and Sterner toxicity classification scale. However, lower oral rat LD50 were estimated for PP4 and PP5: 350 mg/kg and 759 mg/kg, respectively. This toxicity enhancement was also observed for those two photoproducts for the aquatic organisms toxicity tests (fathead minnow LC50 (96 h, mg/L) and Daphnia magna LC50 (48 h, ppm) presented in SI 3. Results of the mutagenicity estimation test were interesting since they exhibited that all the iprodione photoproducts would be mutagenic while the parent compound is not. Indeed iprodione was reported to be non-mutagenic in the literature [36]. The photoproducts expected to be the most mutagenic are PP1 and PP2, which have respectively two and one hydroxyl group(s) on the aromatic ring. This result is coherent with literature data reporting that phenolic groups take part in the mutagenicity observed in mammals [37]. The potential developmental toxicity of iprodione and its photoproducts was also investigated. Results of simulation tests show that iprodione could be responsible for developmental toxicity (see SI 3). This is in agreement with results of a previous study reporting rat pubertal development delay, serum testosterone levels diminution and *ex vivo* testicular testosterone production decreases [38]. Photoproducts PP2 and PP3, which kept the chlorine atoms on the original skeleton, exhibited approximately the same developmental toxicity potential that the parent compound (values between 0.95 and 1.15). The correlation between developmental toxicity of a

Table 1
Retention times, main ions and chemical structures of iprodione and its photoproducts.

Compound	Retention time (min)	Ions (*m*/*z*)	Ion raw formula	Chemical structure
PP1	11.2	294.1076 252.0608 209.0553	$C_{13}H_{16}N_3O_5$ $C_{10}H_{10}N_3O_5$ $C_9H_9N_2O_4$	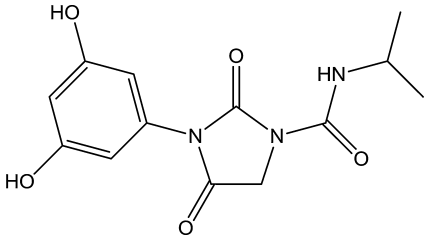
PP2	19.0	312.0739 296.0789 294.1080 270.0270	$C_{13}H_{15}ClN_3O_4$ $C_{12}H_{11}ClN_3O_4$ $C_{13}H_{13}ClN_3O_3$ $C_{10}H_9ClN_3O_4$	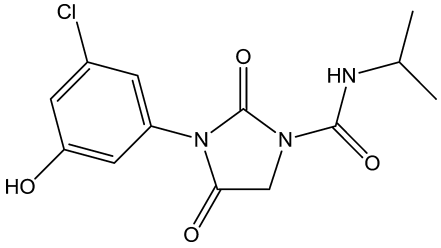
PP3	22.3	296.0789 254.0321 211.0264	$C_{13}H_{15}ClN_3O_3$ $C_{10}H_9ClN_3O_3$ $C_9H_8ClN_2O_2$	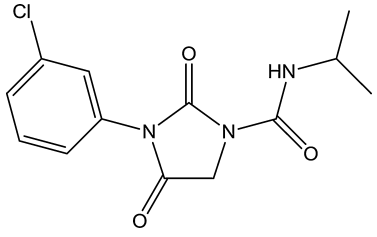
PP4	23.8	330.0399 287.9931 244.9874	$C_{13}H_{14}Cl_2N_3O_3$ $C_{10}H_8Cl_2N_3O_3$ $C_9H_7Cl_2N_2O_2$	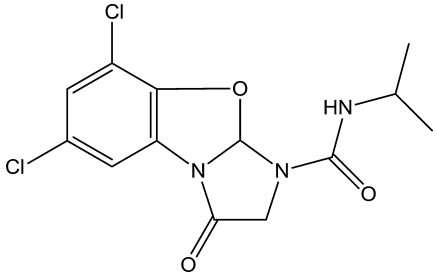
PP5	25.4	330.0399 287.9931 244.9873	$C_{13}H_{14}Cl_2N_3O_3$ $C_{10}H_8Cl_2N_3O_3$ $C_9H_7Cl_2N_2O_2$	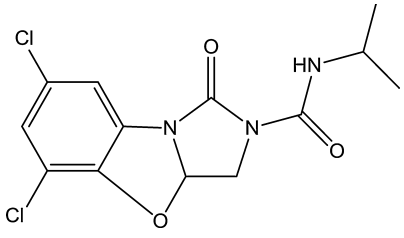
Iprodione	26.2	330.0399 287.9931 244.9873	$C_{13}H_{14}Cl_2N_3O_3$ $C_{10}H_8Cl_2N_3O_3$ $C_9H_7Cl_2N_2O_2$	See Fig. 1

molecule and the presence of chlorine atoms in its chemical structure has been already reported in the literature [39].

Supplementary material related to this article can be found, in the online version, at http://dx.doi.org/10.1016/j.chroma.2014.10.051.

3.3. *In vitro* bioassay results

A reference solution at 10 mg/L and a solution of iprodione at 10 mg/L irradiated for 60 min were tested according to the procedure described in Section 2.7. As presented in Fig. 5, the inhibition percentage after 15 min of incubation shows that the photolyzed solution is clearly more toxic for the marine bioluminescent bacteria than the reference solution. For instance, at a concentration of 10 mg/L, the inhibition percentage is 4 times higher in the photolyzed solution than for the reference one. UV–vis irradiation leads to a significant enhancement of the iprodione solution toxicity. In order to investigate the individual toxicity of each photoproduct, the irradiated solution of iprodione was fractionated; the purity of each fraction was tested by LC–MS and the concentration of each photoproduct was estimated according to the method described in Section 2.5. Estimated concentrations are the following: 1.4, 0.4, 3.4, 0.3 and 2.5 ppm for PP1 to PP5, respectively. They are in good agreement with the chromatographic profile presented in Fig. 2. The *V. fischeri* bioluminescence inhibition test provided EC50 values of 0.3, 0.5, 8.2, 0.4 and 1.3 ppm for PP1 to PP5, respectively. The EC50 value for iprodione was estimated greater than 10 ppm but could not be accurately determined for solubility reasons. All

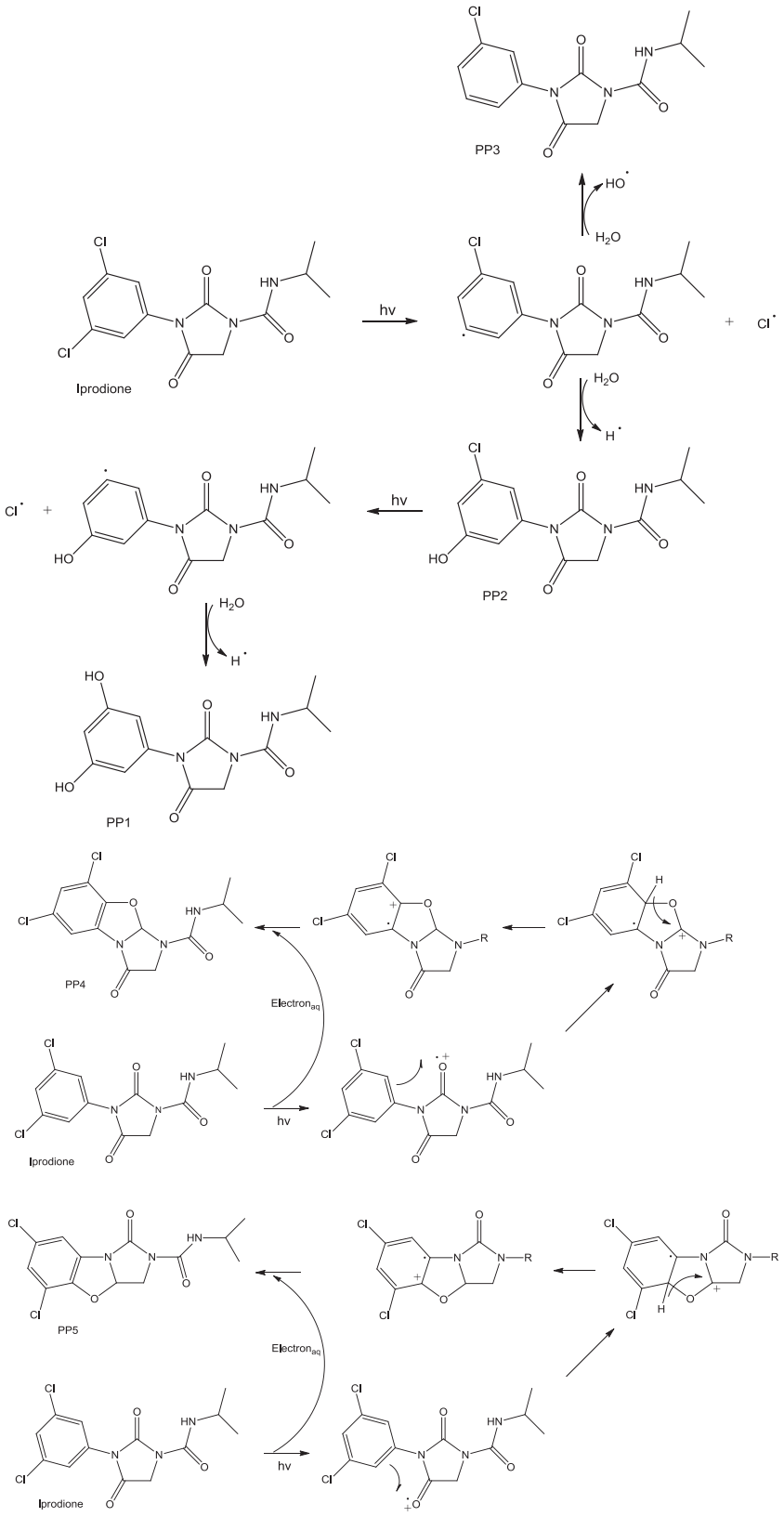

Fig. 3. Suggested transformation pathways of iprodione under UV–vis irradiation.

photoproducts are thus more toxic than the parent molecule. High toxicity values for PP1 and PP2 were expected given than numerous phenolic compounds are known to exhibit a significant toxicity. The low EC50 value (0.4 ppm) determined for PP4 is more surprising especially compared to that of the other cyclic isomer of iprodione PP5. Given its high relative abundance and its low EC50 value, the detection of PP1 will be prioritized in real samples as soon as there are some available.

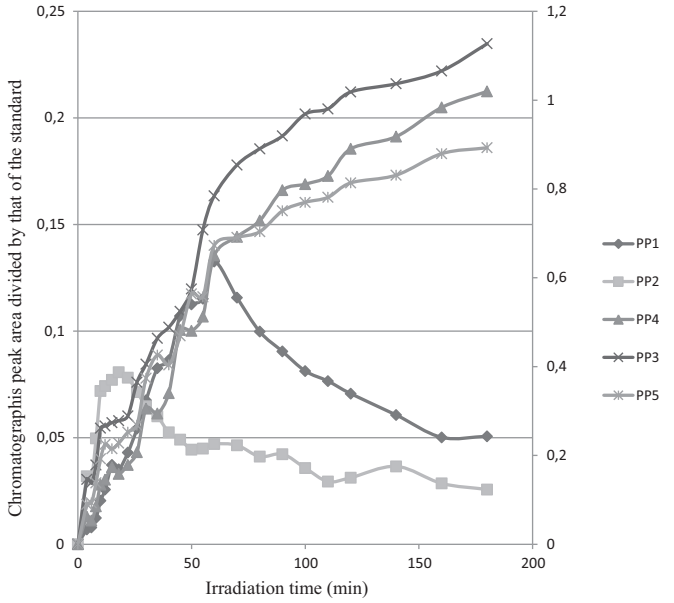

Fig. 4. Relative amounts of photoproducts of iprodione plotted as a function of the irradiation time (the left vertical axis is used for PP1, PP2 and PP4 while the right one is used for PP3 and PP5).

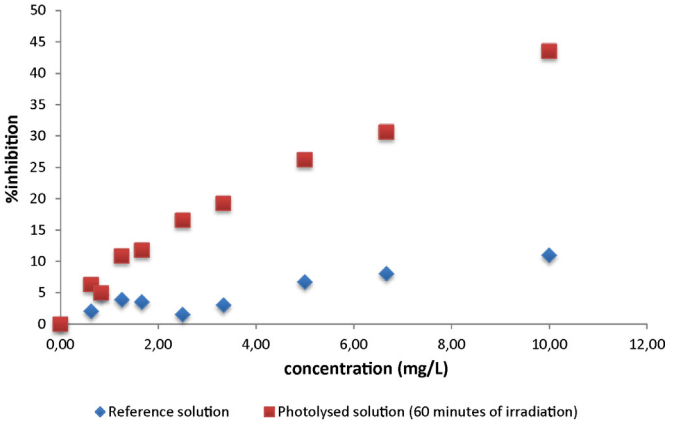

Fig. 5. Response–dose curves for both reference and photolyzed iprodione solutions with the *Vibrio fischeri* bioluminescence inhibition test.

4. Conclusion

Five photoproducts of iprodione were characterized by LC–MS; none of them has been reported in previous studies. Three photoproducts result from elimination of one or two chlorine atoms followed by hydroxy or hydrogen addition while two products are cyclic isomers of iprodione. Photo transformation pathways were suggested to rationalize their formation. *In silico* toxicity predictions showed that cyclized photoproducts are potentially more toxic than the parent compound considering oral rat LD50 while phenolic photoproducts induce the major mutagenicity. Photoproducts having kept a chlorine atom are expected to induce a potential developmental toxicity comparable to that of iprodione. *In vitro* assays on *V. fischeri* showed that an aqueous iprodione solution is significantly more toxic after irradiation than before. Sample fractionation permitted to establish that phenolic compounds are mainly responsible for toxicity enhancement with EC50 values of 0.3 and 0.5 ppm, for the bi- and mono-phenolic compounds issued from chlorine elimination, respectively. In a recent study devoted to boscalid phototransformation, we showed that some photoproducts produced under laboratory conditions were detected in Lebanon real grape samples [40]. In the present work, no real environmental sample submitted to solar irradiation under field conditions was available. Grape berries treated with a commercial preparation of iprodione were submitted to irradiation under laboratory conditions and photoproducts were detected in both skin and flesh of berries after they have been rinsed with water. These results do not provide proof that these photoproducts would be formed under field conditions nor that they would be persistent enough to induce acute toxicity. Nevertheless, particular attention should be paid to fruits treated with iprodione and submitted to intense and/or long sunshine exposure.

Acknowledgments

Financial supports from the National FT-ICR network (FR 3624 CNRS) and from the *Ile de France Région* for conducting the research are gratefully acknowledged.

References

[1] A. Grube, D. Donaldson, T. Kiely, L. Wu, U.S. Environmental Protection Agency, EPA-733-R-11-001, 2011.
[2] V. Morton, T. Staub, Online, APSnet Features, 2008, doi 10.1094.
[3] A.E.S. Perez, R.M. Valdebenito-Sanhueza, V. Duarte, H.P. Santos, J. Felippeto, Controle do mofo cinzento com Clonostachys rosea na produção de mudas de fúcsia, Trop. Plant Pathol. 35 (2010) 163–169.
[4] J. Northover, J. Matteoni, Resistance of *Botrytis cinerea* to Benomyl and Iprodione in vineyards and greenhouses after exposure to the fungicides alone or mixed with captan, Plant Dis. 70 (1986) 398–402.
[5] C. Turgut, H. Ornek, T.J. Cutright, Pesticide residues in dried table grapes from the Aegean region of Turkey, Environ. Monit. Assess. 167 (2010) 143–149.
[6] R. Beever, E. Laracy, H. Pak, Strains of *Botrytis cinerea* resistant to dicarboximide and benzimidazole fungicides in New Zealand vineyards, Plant Pathol. 38 (1989) 427–437.
[7] W. Yi, S.E. Law, H.Y. Wetzstein, Pollen tube growth in styles of apple and almond flowers after spraying with pesticides, J. Horticult. Sci. Biotechnol. 78 (2003) 842–846.
[8] A. Angioni, L. Porcu, F. Dedola, Determination of famoxadone, fenamidone, fenhexamid and iprodione residues in greenhouse tomatoes, Pest. Manag. Sci. 68 (2012) 543–547.
[9] M. Omirou, Z. Viyzas, E. Papadopoulou-Mourkidou, A. Economou, Dissipation rates of iprodione and thiacloprid during tomato production in greenhouse, Food Chem. 116 (2009) 499–504.
[10] J. Strömqvist, N. Jarvis, Sorption, degradation and leaching of the fungicide iprodione in a golf green under Scandinavian conditions: measurements, modelling and risk assessment, Pest. Manag. Sci. 61 (2005) 1168–1178.
[11] E.-H. Pommer, G. Lorenz, Dicarboximide fungicides, in: H. Lyr (Ed.), Modern Selective Fungicides, Gustav Fischer, 1987, pp. 99–118.
[12] C.R. Blystone, C.S. Lambright, J. Furr, V.S. Wilson, L.E. Gray Jr., Iprodione delays male rat pubertal development, reduces serum testosterone levels, and decreases ex vivo testicular testosterone production, Toxicol. Lett. 174 (2007) 74–81.
[13] EPA, MRID 42637801, 1992.
[14] Health & Consumer Protection Directorate-General, Review report for the active substance iprodione 5036/VI/98-final, 2002.
[15] L. Maltby, T.C.M. Brock, P.J. van den Brink, Fungicide risk assessment for aquatic ecosystems: importance of interspecific variation, toxic mode of action, and exposure regime, Environ. Sci. Technol. 43 (2009) 7556–7563.
[16] S. Milenkovski, E. Baath, P.E. Lindgren, O. Berglund, Toxicity of fungicides to natural bacterial communities in wetland water and sediment measured using leucine incorporation and potential denitrification, Ecotoxicology 19 (2010) 285–294.
[17] T. Katagi, Photodegradation of pesticides on plant and soil surfaces, Rev. Environ. Contam. Toxicol. 182 (2004) 1–189.
[18] H.D. Burrows, M. Canle, J.A. Santaballa, S. Steenken, Reaction pathways and mechanisms of photodegradation of pesticides, J. Photochem. Photobiol. 67 (2002) 71–108.
[19] W. Schwack, B. Bourgeois, F. Walker, Fungicides and photochemistry photodegradation of the dicarboximide fungicide iprodione, Chemosphere 31 (1995) 2993–3000.
[20] D. Mueller, Fungicides: Plant Health Fungicide Applications, vol. 496, Iowa State Univ. Integrated Crop Management, 2006, pp. 122–127.
[21] I. Yamaguchi, M. Fujimura, Recent topics on action mechanisms of fungicides, J. Pest. Sci. 30 (2005) 67–74.
[22] S. Zapf, K. Klappach, J. Pfenning, M.K. Ernst, Erarbeitung eines Testverfahrens zur Bestimmung der Protektiv- und Kurativleistung von Fungiziden bei der Bekämpfung des Erregers der Stemphylium-Laubkrankheit Stemphylium botryosum in der Spargelkultur (*Asparagus officinalis* L.), Gesunde Pflanz 63 (2011) 167–174.

[23] K. Hustert, P.N. Moza, Photochemical degradation of dicarboximide fungicides in the presence of soil constituents, Chemosphere 35 (1997) 33–37.
[24] B. Schick, P.N. Moza, K. Hustert, A. Kettrup, Photochemistry of vinclozolin in water and methanol–water solution, Pestic. Sci. 55 (1999) 1116–1122.
[25] A. Rifai, Y. Souissi, C. Genty, C. Clavaguera, S. Bourcier, F. Jaber, S. Bouchonnet, Ultraviolet degradation of procymidone – structural characterization by gas chromatography coupled with mass spectrometry and potential toxicity of photoproducts using *in silico* tests, Rapid Commun. Mass Spectrom. 27 (2013) 1505–1516.
[26] A.M. Wightwick, A.D. Bui, P. Zhang, G. Rose, M. Allinson, J.H. Myers, S.M. Reichman, N.W. Menzies, V. Pettigrove, G. Allinson, Investigation of 25 fungicides in surface waters of a horticultural production catchment in south-eastern Australia, Arch. Environ. Contam. Toxicol. 62 (2012) 380–390.
[27] Y. Picó, M. Farré, C. Soler, D. Barceló, Confirmation of fenthion metabolites in oranges by IT-MS and QqTOF-MS, Anal. Chem. 79 (2007) 9350–9363.
[28] Y. Picó, M. Farré, C. Soler, D. Barceló, Identification of unknown pesticides in fruits using ultra-performance liquid chromatography-quadrupole time-of-flight mass spectrometry. Imazalil as a case study of quantification, J. Chromatogr. A 1176 (2007) 123–134.
[29] A. Masiá, J. Campo, C. Blasco, Y. Picó, Ultra-high performance liquid chromatography-quadrupole time-of-flight mass spectrometry to identify contaminants in water: an insight on environmental forensics, J. Chromatogr. A 1345 (2014) 86–97.
[30] http://www.biomonitoring.ca.gov/sites/default/files/downloads/0709 Iprodione.pdf
[31] M. Ashley, ROMIL Technical Report, ROMIL, Cambridge, GB-CB5 9QT, 2006 www.romil.com
[32] USEPA, Final Contaminant Candidate List 3 Chemicals: Identifying the Universe, U.S. Environmental Protection Agency, 2009, available from: http://www.epa.gov/safewater/ccl/ccl3.html#chemical
[33] L.H. Hall, B. Mohney, L.B. Kier, The electrotopological state: structure information at the atomic level for molecular graphs, J. Chem. Inf. Comput. Sci. 31 (1991) 76–82.
[34] K. Takehara, M. Itabashi, K. Hayashi, S. Kudow, A. Kawakubo, M. Tajima, Acute toxicity of Rovral (26019RP) I. Oral, intraperitoneal and subcutaneous administration in mice, 1976.
[35] http://www.fao.org/fileadmin/templates/agphome/documents/Pests_Pesticides/Specs/Iprodione06.pdf
[36] United States Prevention, Pesticides EPA-738-F-98-017 Environmental Protection and Toxic Substances Agency (7508C), November 1998.
[37] P.G. Wislocki, A.W. Wood, R.L. Chang, W. Levin, H. Yagi, O. Hernandez, P.M. Dansette, D.M. Herina, A.H. Conney, Mutagenicity and cytotoxicity of benzo(a)pyrene arene oxides, phenols, quinones, and dihydrodiols in bacterial and mammalian cells, Cancer Res. 36 (1976) 3350–3357.
[38] C.R. Blystone, C.S. Lambright, J. Furr, V.S. Wilson, L.E. Gray, Environmental pollutants and dysregulation of male puberty – a comparison among species, Toxicol. Lett. 174 (2007) 74–81.
[39] M. Yang, X. Zhang, Comparative developmental toxicity of new aromatic halogenated DBPs in a chlorinated saline sewage effluent to the marine polychaete *Platynereis dumerilii*, Environ. Sci. Technol. 47 (2013) 10868–10876.
[40] Y. Lassale, A. Kinani, A. Rifai, Y. Souissi, C. Clavaguera, S. Bourcier, F. Jaber, S. Bouchonnet, UV-visible degradation of boscalid – structural characterization of photoproducts and potential toxicity using *in silico* tests, Rapid Commun. Mass Spectrom. 28 (11) (2014) 53–63.